Journal of Renewable Materials

Evaluation of Mechanical Properties of Cross-Laminated Timber with Different Lay-ups Using Japanese Larch

Yingchun Gong[1,#,*], Fenglu Liu[2,#], Zhaopeng Tian[1], Guofang Wu[1], Haiqing Ren[1] and Cheng Guan[2]

[1]Research Institute of Forestry New Technology, Chinese Academy of Forestry, Beijing, 100091, China.

[2]School of Technology, Beijing Forestry University, Beijing, 10083, China.

[#]These authors contributed to the work equally and should be regarded as co-first authors.

[*]Corresponding Author: Yingchun Gong. Email: gongyingchun@caf.ac.cn.

Abstract: Japanese larch is one of the main plantation tree species in China. A lack of engineered wood products made by Japanese larch, however, limits its application in wood structures. In this study, based on optimum process parameters, such as pressure (1.2 MPa), adhesive spread rate (200 g/m^2) and adhesive (one-component polyurethane), the mechanical properties of Japanese larch-made cross-laminated timber (CLT) with different lay-ups were evaluated by means of the static method. Results of this study showed that variations in lay-ups significantly affected the mechanical properties of CLT. The strength and modulus of bending and parallel compression for CLT increased with the thickness of lumber, while that of bending, parallel compression and rolling shear all decreased with the number of layers. Thickness, layup orientation and the number of layers all had an impact on the strength of CLT. Failure modes obtained from numerical simulation were basically the same as those of experimental tests. There was also strong alignment between theoretical value and test value for effective bending stiffness and shear stiffness. Thus, the shear analogy method can be used to predict the mechanical properties of CLT effectively. This study proved great potential in using Japanese larch wood for manufacturing CLT due to its good mechanical properties.

Keywords: Cross-laminated timber; mechanical properties; lay-ups; failure mode; shear analogy

1 Introduction

Cross-laminated timber (CLT) is a prefabricated engineered wood product dedicated to structural applications. CLT is created from layers of sawn lumber or structural composite lumber orthogonally bonded by adhesive, nails, or wooden dowels [1-6]. Compared with other engineered wood products, CLT is lighter, boasting superior acoustic, fireproof, seismic, and thermal performance, with widespread use for roofs, floors, and walls in residential and non-residential construction [7-10]. Spruce-pine-fir and Norway spruce are common species for CLT manufactured in North America and Europe [11]. Due to the logging ban on natural forests implemented in China since 2015, wood resources have seen a serious shortage, making it necessary for the country to develop and utilize plantation forests [12]. As one of the main plantation species in China, Japanese larch (*Larix kaempferi Carr.*) is widely distributed from 35° to 38° N and 136° to 140° E. But, a lack of engineered wood products made by this species limits its application in building structures. Therefore, it is significant to explore CLT made by Japanese larch, in a move to use such a green and sustainable material in buildings and timber structures.

Previous studies were mainly focused on the bending strength, rolling shear strength, numerical model, and connection performance of CLT [13-15]. Due to the anisotropic properties of wood, rolling shear strength in the radial-tangential (RT) plane is much lower than in the longitudinal-radial (LR) or longitudinal-tangential (LT) plane [16]. Currently, rolling shear stiffness and strength must be considered in applications of conventional CLT under certain loading ways due to the existence of cross-layers [17]. For example, CLT floor panels with highly concentrated loads in supported areas may cause high rolling shear stress in cross layers. The same may also happen to short-span floors or beams under out-of-plane bending loads [18]. Therefore, it is meaningful to improve rolling shear properties by changing the lay-ups of CLT.

In China, lots of planted Japanese larches have grown to useful timber in Liaoning, Hubei and Sichuan provinces, among other places. The purpose of this study was to evaluate the mechanical properties of CLT in different lay-ups manufactured with fast-growing Japanese larch. These properties, i.e., strength and modulus of bending, rolling shear and parallel compression were evaluated by using static testing and analytical methods. This study will provide basic data for the application of Japanese larch-made CLT in the building sector, as part of efforts to promote the development of high-rise construction.

2 Materials and Methods

2.1 Materials

Japanese larch was harvested from the Ying'emen National Plantation, located in Ying'emen Town, Liaoning Province, China (125.2° E, 42.2° N, at an altitude of approximately 877 meters). A total of 2,000 lumbers with dimensions of 25 mm (thickness) × 90 mm (width) × 2,700 mm (length) were cut from 351 three-meter-long logs with a diameter ranging from 250 mm to 320 mm. Then they were dried in a kiln, after which, the density and moisture content of those lumbers was tested in the lab, the former standing at 0.597 g/cm^3 ± 0.035 g/cm^3, and the latter being 12% ± 0.96%. Lumbers were classified into three grades (low, middle and high) based on their dynamic modulus of elasticity (MOE), determined by stress wave technique using Fakopp Microsecond Meter (Fakopp Enterprise, Hungary). Lumbers with a dynamic MOE ranging from 12,000 to 16,000 MPa and 8,000 to 12,000 MPa were selected as the parallel layers and the perpendicular layers of CLT, respectively.

Based on the optimum process parameters [12], generally including pressure (1.2 MPa), adhesive spread rate (200 g/m^2), and adhesive (one-component polyurethane), four types of CLT varying in layup were manufactured, including orthogonally bonded three-layer CLTs with 75 mm and 45 mm thickness (3-layer-75, 3-layer-45), orthogonally bonded five-layer CLT with 75 mm thickness (5-layer-75) and alternating 90° parallel layers and ± 45° transverse-layer CLT with 75 mm thickness (5-45°-layer-75). CLT panels were manufactured on an industrial CLT production line in Ningbo Sino-Canada Low-Carbon Technology Research Institute Co. Ltd. Their size was shown in Tab. 1.

Table 1: Size of four CLT types varying in layup

CLT Types	Numbers	Parameters		
		Length (mm)	Width (mm)	Thickness (mm)
3-layer-75	3	2,800	1,340	75
3-layer-45	3	2,800	1,318	45
5-layer-75	3	2,800	1,340	75
5-45°-layer-75	3	2,800	1,340	75

2.2 Static Testing Method

2.2.1 Sampling

Specimen sampling patterns in CLT for static testing were plotted in Fig. 1. To ensure that samples cut from CLT were sufficiently random, three different sawing patterns (as shown in Figs. 1(a)-1(c), respectively) were used to obtain enough and satisfactory specimens for static tests.

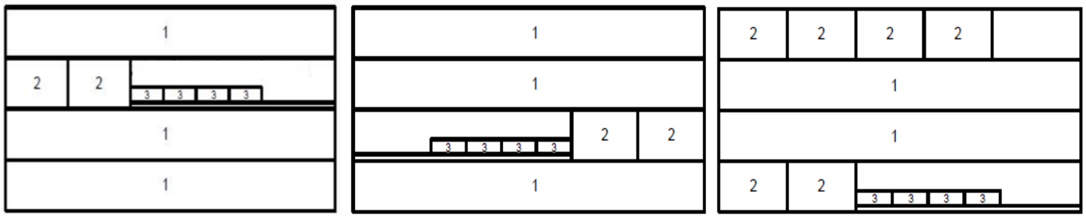

(a) (b) (c)

Figure 1: Schematic diagram of: (a) the first sawing pattern, (b) the second sawing pattern, (c) the third sawing pattern of samples

Number 1 in Fig. 1 represents sawing location of specimens for bending tests. Likewise, Number 2 and 3 indicate sampling location of specimens for rolling shear and parallel compressive tests, respectively. Tab. 2 shows the size of samples for mechanical properties testing.

Table 2: Size of specimen for mechanical properties testing

Mechanical properties test	Size (mm) (Length × width × thickness)	Number of specimens
Bending	2,700 (parallel to grain) × 305 × 75	8 × 3
	2,700 (parallel to grain) ×305 × 45	8
Rolling shear	510 (parallel to grain) × 305 × 75	12 × 3
	510 (parallel to grain) × 305 × 45	12
Parallel compression	270 (parallel to grain) × 90 × 75	12 × 3
	270 (parallel to grain) × 90 × 45	12

2.2.2 Bending Tests

To evaluate the bending properties of CLT, three-point bending tests were carried out on an MTS universal testing machine according to ANSI/APA PRG 320-2017 [19]. Specimens were loaded at a rate of 5 mm/min. The span-to-depth ratio for specimens was 30. It should be noted that the span for 75 mm-thick CLT was different from that for 45 mm-thick CLT in bending tests. Therefore, in order to maintain the same ratio, i.e., 30, in bending tests, the span of 75 mm-thick CLT was set to 2,250 mm, and then the span of 45 mm-thick CLT at 1,350 mm. Modulus of elasticity ($E_{b,CLT}$) and bending strength ($f_{b,CLT}$) were calculated from Eqs. (1) and (2), respectively.

$$E_{b,CLT} = \frac{23\Delta p l^3}{108\Delta y b h^3} \tag{1}$$

$$f_{b,CLT} = \frac{F_{b,\max} l}{b h^2} \tag{2}$$

where l is the span of specimen (mm); b is the width of test specimen (mm); h is the thickness of test specimen (mm); $\Delta p/\Delta y$ is relationship between changes in load and deformation; $F_{b,max}$ is maximum load for bending tests (N). The range of maximum load was between 22 kN and 49 kN.

2.2.3 Rolling Shear Tests

Rolling shear performance is an important indicator for evaluating the mechanical properties of CLT, as well as the key to designing and applying CLT products. In terms of ASTM D198-02 [20], center-point bending tests were conducted on rolling shear samples to estimate such properties. Specimens were loaded at a rate of 1 mm/min on an Instron 5582 machine. The span-to-depth ratio for specimens was 6. Similar to bending tests, the span for 75 mm-thick CLT was different from that for 45 mm-thick CLT in rolling shear tests. Therefore, the span of 75 mm-thick CLT was 450 mm, and the span of 45 mm-thick CLT was 270 mm to ensure the same ratio, i.e., 6. Rolling shear modulus(G) and strength(τ_{CLT}) were calculated using Eqs. (3) and (4), respectively.

$$\frac{1}{E_{m,app}}=\frac{1}{E_m}+\frac{1}{KG}(\frac{h}{l})^2 \tag{3}$$

$$\tau_{CLT}=\frac{3F_{\tau,\max}}{4bh} \tag{4}$$

where Em, app is the apparent modulus of elasticity that incorporates the influence of shear deformation (MPa); Em is the true modulus of elasticity (MPa); K is shear coefficient (K equals 0.84 for rectangular section); Fτ, max is the maximum load for rolling shear tests (N).

2.2.4 Parallel Compression Tests

YAW-3000A, a microcomputer controlled electro-hydraulic servo pressure testing machine, was used to perform parallel compression tests on the basis of ASTM 4761 [21]. The loading speed of specimen for compression tests was 2 mm/min. The modulus of elasticity (Ec,0,CLT) and parallel compression strength (fc,0,CLT) were then obtained from Eqs. (5) and (6), respectively.

$$E_{c,0,CLT}=\frac{\Delta p}{\Delta y}\cdot\frac{1}{bh} \tag{5}$$

$$f_{c,0,CLT}=\frac{F_{c,0,\max}}{bh} \tag{6}$$

where b is width of test specimen (mm); h is thickness of test specimen (mm); $\Delta p/\Delta y$ is relationship between changes in load and deformation; $F_{c,0,max}$ is the maximum load for parallel compression tests (N).The range of maximum load was between 161 kN and 319 kN.

2.3 Numerical Simulation

Numerical simulation was adopted to verify the validity of static test experiments, with the expectation that the mechanical properties of CLT can be predicted by simulation. ABAQUS software was the tool to simulate the mechanical properties of CLT structure. Three types of CLT model, namely, 3-layer-75, 5-layer-75 and 5-45-layer-75, were established by using C3D8R elements in ABAQUS. The C3D8R element is an eight-node linearly reduced integral three-dimensional solid element. Each node in the C3D8R element has three degrees of freedom in translation at the x, y, and z directions [22,23]. The simulation model of CLT had identical dimensions with actual CLT, and the thickness of a single layer for simulation was 25 mm. The dimensions of CLT model built in ABAQUS were 2,700 × 305 × 75 mm, 510 × 305 × 75 mm and 270 × 305 × 75 mm for bending, rolling shear and parallel compression, respectively. CLT was considered an orthotropic material in numerical simulation, and the elastic constants used to define its properties were measured through the resistance strain gauges method, widely recognized as a general way for testing the static mechanical properties of wood [24-27] in laboratory. The elastic constants for the parallel layers and the perpendicular layers of CLT model were given in Tab. 3 and Tab. 4, respectively.

Table 3: Elastic constants for the parallel layers of CLT model

Modulus of elasticity (MPa)		Modulus of rigidity (MPa)		Poisson's ratio	
E_L^1	13860	G_{RT}^4	180	$_{LR}^{7}$	0.362
E_R^2	1208	G_{LR}^5	716	$_{LT}^{8}$	0.419
E_T^3	1105	G_{LT}^6	312	$_{RT}^{9}$	0.662

[1]E_L-longitudinal modulus of elasticity; [2]E_R-radial modulus of elasticity; [3]E_T-tangential modulus of elasticity;
[4]G_{RT}-shear modulus in R-T plane; [5]G_{LR}-shear modulus in L-R plane; [6]G_{LT}-shear modulus in L-T plane;
[7]υ_{LR}, [8]υ_{LT}, [9]υ_{RT} -Poisson's ratio

Table 4: Elastic constants for the perpendicular layer of CLT model

Modulus of elasticity (MPa)		Modulus of rigidity (MPa)		Poisson's ratio	
E_L	10330	G_{RT}	137	$_{LR}$	0.578
E_R	1083	G_{LR}	666	$_{LT}$	0.591
E_T	962	G_{LT}	250	$_{RT}$	0.614

To prevent stress concentration and additional deformation of CLT model, a 100 mm (length) × 305 mm (wide) support surface and a reference point were coupled at the support location (see Fig. 2(a)). Then, constraints were set at the reference point. This meant that displacement in x, y, z directions at one end and x, z directions at the other end of CLT model was constrained.

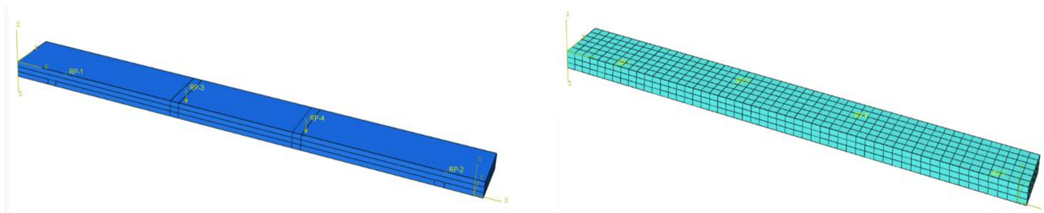

(a) (b)

Figure 2: Schematic diagram of: (a) couple of support surface and reference point, (b) applied constraints

Moreover, in order to prevent torsion in model, the rotation of the reference point around y axis was constrained, as shown in Fig. 2(b). Load was only applied to matrix material. The dynamic and explicit analysis method was used to solve the model to obtain stress and strain maps of CLT.

2.4 Analytic Approach

Being applicable to any loading method, shear analogy theory has become the most widely used in CLT theoretical calculations. The influence of rolling shear modulus between layers on bending performance is considered in this theory. Effective bending stiffness (EI)eff and shear stiffness (GA)eff of 3-layer-75, 3-layer-45 and 5-layer-75 CLT were calculated by Eqs. (8) and (9), respectively, according to the shear analogy method.

$$(EI)_{eff} = (EI)_A + (EI)_B = \sum_{i=1}^{n} E_i \cdot b_i \cdot \frac{h_i^a}{12} + \sum_{i=1}^{n} E_i \cdot A_i \cdot Z_i^2 \tag{8}$$

$$(GA)_{eff} = \frac{a^2}{\left[\left(\frac{h_1}{2 \cdot G_1 \cdot b}\right) + \left(\sum_{i=2}^{n-1} \frac{h_i}{G_i \cdot b}\right) + \left(\frac{h_n}{2 \cdot G_n \cdot b}\right) \right]} \tag{9}$$

where Ei is the modulus of elasticity of layer i (MPa), Ei (i = 1,3,5) equals 13,860 MPa and Ei (i = 2,4) equals 10,330 MPa; Ai is the cross-sectional area of layer i (mm^2); bi is the width of layer i (mm); hi is the thickness of layer i (mm); Zi is the distance between the center point of layer i and the neutral axis (mm), and Gi is the rolling shear modulus of layer i (MPa). The rolling shear modulus GR is assumed to be 1/10 of the shear modulus parallel to the grain and the boards, G0. G0 is generally assumed to be 1/16 of the modulus of elasticity (Ei) for softwood lumber [8].

3 Results and Discussion

3.1 Mechanical Properties

3.1.1 Bending Modulus and Strength

The mechanical properties of measured CLT with different lay-ups were shown in Tab. 5. The bending modulus for CLT made from Japanese Larch ranged from 11.38 GPa to 13.36 GPa, and the bending strength from 44.14 MPa to 55.83 MPa. Previous research revealed that the bending modulus of

CLT with three layers of layup using hybrid poplars ranged from 9.7 GPa to 11.6 GPa, and the bending strength varied from 35.37 MPa to 48.19 MPa [28,29], obviously lower than the values computed in this study. This may show that CLT produced from Japanese Larch had greater bending properties than from hybrid poplars.

Table 5: Results of mechanical properties for CLT with different lay-ups

CLT	Bending modulus		Bending strength		Rolling shear modulus		Rolling shear strength		Compressive modulus		Compressive strength	
	Mean (GPa)	COV (%)	Mean (MPa)	COV (%)	Mean (MPa)	COV (%)	Mean (MPa)	COV (%)	Mean (MPa)	COV (%)	Mean (MPa)	COV (%)
[1]3-layer-75	13.06	3.74	51.58	11.10	146.69	18.35	2.54	8.53	9.60	19.17	39.83	10.69
[2]3-layer-45	13.36	5.54	55.83	10.60	143.28	17.58	3.16	4.42	10.04	18.27	41.72	8.45
[3]5-layer-75	11.38	4.24	44.14	7.47	137.67	12.61	2.33	7.99	9.10	15.86	34.31	6.3
[4]5-45°-layer-75	11.80	2.73	46.01	10.90	172.01	14.32	3.37	8.78	10.54	20.28	39.61	8.48

For bending properties, as shown in Tab. 5, 3-layer-45 CLT had the highest bending modulus and strength, about 17.39% and 26.48% higher than those of 5-layer-75 CLT, respectively. The number of layers of CLT being the same, the bending strength and modulus of CLT slightly increased by 8.24% and 2.30%, respectively, as the thickness of timber decreased from 25 mm to 15 mm. While the thickness of timber was identical, the bending strength and modulus of CLT decreased by 20.94% and 14.82% respectively as the layer numbers increased from 3 to 5. Different with the orthogonal five-layer CLT, in addition, the bending strength and modulus of CLT with 45° layers mildly increased by 4.24% and 3.69%, respectively. This may be due to the fact that for 5-45°-layer-75 CLT the force acting on the middle layer was between the transverse load and the parallel load. Therefore, compared with the transverse layer of the orthogonal CLT, the middle layer of 5-45°-layer-75 CLT can resist part of bending moment. Ultimately, the bending modulus and strength of 5-45°-layer-75 CLT were increased.

Table 6: Analysis of variance of mechanical performance for CLT

Difference source		Sum of squares	Degree of freedom	Mean square	*f* value	*p* value
Bending modulus	Between groups	26.99	3	8.99	31.93	3.99×10^{-10}
	Within groups	9.86	28	0.28		
	Total	36.86	31			
Bending strength	Between groups	639.28	3	213.09	8.31	4.48×10^{-4}
	Within groups	692.43	28			
	Total	1,331.71	31			
Rolling shear modulus	Between groups	5,621.21	3	1873.74	3.82	0.019
	Within groups	14,710.82	28	490.36		
	Total	20,332.03	31			
Rolling shear strength	Between groups	6.73	3	2.24	54.36	8.48×10^{-12}
	Within groups	1.16	28	0.041		
	Total	7.89	31			
Compressive modulus	Between groups	14.64	3	4.88	1.46	0.24
	Within groups	146.60	44	3.33		
	Total	161.24	47			
Compressive strength	Between groups	375.37	3	125.12	11.82	8.29×10^{-6}
	Within groups	465.62	44	10.58		
	Total	840.99	47			

To investigate the effect of thickness, number of layers and lay-up on the mechanical performance of CLT, analysis of variance and least significant differences were conducted on the measured data. The analysis results were presented in Tab. 6 and Tab. 7, respectively. It was patently observed from Tab. 6

that lay-up had a prominent impact on both the bending modulus and strength of CLT ($p < 0.05$).

Moreover, Tab. 7 showed that only the number of layers significantly influenced bending modulus and strength. In other words, the study found no remarkable difference in bending performance resulting from thickness and layup orientation. This may be attributable to the fact that the transverse layer was far away from the central axis of CLT as the number of layers increased, and then the moment of inertia of the transverse section was weakened. Therefore, the bending modulus and strength of CLT were decreased.

Table 7: Analysis of least significant difference of mechanical performance for CLT

Difference source		Mean difference	Standard error	*p* values	95% confidence interval	
					Lower limit	Upper limit
Bending modulus	#1[1] and #2[2]	0.30	0.24	0.23	-0.19	0.79
	#2 and #3[3]	-1.98	0.24	8.23×10^{-10}	-2.46	-1.49
	#3 and #4[4]	0.42	0.24	0.084	-0.060	0.90
Bending strength	#1 and #2	4.24	2.62	0.12	-1.13	9.62
	#2 and #3	-11.68	2.62	1.31×10^{-4}	-17.06	-6.31
	#3 and #4	1.86	2.53	0.47	-3.34	7.06
Rolling shear modulus	#1 and #2	-3.42	10.50	0.75	-24.87	18.03
	#2 and #3	-9.02	11.07	0.42	-31.63	13.59
	#3 and #4	34.33	11.07	0.0042	11.72	56.94
Rolling shear strength	#1 and #2	0.56	0.10	7.20×10^{-6}	0.35	0.77
	#2 and #3	-0.83	0.10	6.19×10^{-9}	0.69	1.10
	#3 and #4	1.17	0.10	3.88×10^{-12}	0.96	1.38
Compressive modulus	#1 and #2	0.61	0.75	0.41	-0.89	2.12
	#2 and #3	-1.21	0.75	0.11	-2.71	0.29
	#3 and #4	1.41	0.75	0.065	-0.092	2.91
Compressive strength	#1 and #2	3.24	1.33	0.019	0.57	5.92
	#2 and #3	-7.73	1.33	6.19×10^{-7}	-10.41	-5.05
	#3 and #4	5.31	1.33	2.41×10^{-4}	2.63	7.99

[1]#1, 3-layer-75 CLT; [2]#2, 3-layer-45 CLT; [3]#3, 5-layer-75; [4]#4, 5-45-layer-75 CLT

3.1.2 Rolling Shear Modulus and Strength

As shown in Tab. 5, the rolling shear modulus of CLT varied from 137.67 MPa to 172.01 MPa, and the rolling shear strength from 2.33 MPa to 3.37 MPa. Studies have indicated that the rolling shear modulus for Spruce CLT, SPF CLT, and CLT fabricated with yellow birch and aspen ranged from 40 MPa to 80 MPa [30], 48 MPa to 83 MPa, and 161 MPa to 193 MPa [31], respectively. This suggested that Japanese Larch as perpendicular layers could significantly improve the rolling shear modulus compared to SPF and Spruce. Wang et al. investigated into the improvement in the rolling shear strength by using composite structure material or modified fast-growing poplar as the perpendicular layer [32]. Gu and Pang calculated the rolling shear strength of southern Pine CLT with different adhesives, which ranged from 1.69 MPa to 2.43 MPa [33]. Besides, Wang et al. determined the mean rolling shear modulus and characteristic rolling shear strength values of the poplar wood, i.e., 177 MPa and 2.24 MPa, respectively [34]. Therefore, the rolling shear strength obtained in this study was similar to previous research findings.

Furthermore, Tab. 5 revealed that the rolling shear strength and modulus of CLT with 45° layers were higher than CLT of other lay-ups. For instance, the value was about 44.64% and 24.94%, respectively, higher than that of 5-layer-75 CLT. In addition, thickness being the same, rolling shear modulus and strength decreased by 4.07% and 35.62%, respectively, as the number of layers increased from 3 to 5. Analysis of variance for mechanical characteristics of CLT (Tab. 6) suggested that layup had a significant impact on the rolling shear modulus and strength. According to the results from analysis of least significant difference (given in Tab. 7), it could be concluded that only layup orientation showed a noticeable influence on rolling shear modulus. This may have to do with the fact that the middle layer of 5-45°-layer-75 CLT can resist part of the bending moment. Consequently, the bending modulus of

5-45°-layer-75 CLT was increased. It meant that the rolling shear modulus of CLT could be improved by changing layup orientation. However, besides layup orientation, thickness and the number of layers both had a dominating impact on rolling shear strength. It was probably due to the truth that the macroscopic defects of wood increased with thickness and the number of layers. And then the mechanical properties of CLT decreased.

3.1.3 Parallel Compressive Modulus and Strength

As can be seen in Tab. 5, the parallel compressive modulus of CLT varied from 9.10 MPa to 10.54 MPa, and the parallel compressive strength from 34.31 MPa to 39.61 MPa. The number of layers being the same, the parallel compressive modulus and strength of CLT slightly increased by 4.85% and 4.75%, respectively, as the thickness of timber decreased from 25 mm to 15 mm. While the thickness of timber was identical, the parallel compressive modulus and strength of CLT decreased by 9.36% and 17.76% respectively as the layer numbers increased from 3 to 5. Compared with the orthogonal five-layer CLT, in addition, the parallel compressive modulus and strength of CLT with 45° layers visibly increased 15.82% and 15.45%, respectively.

Additionally, analysis of variance for mechanical characteristics of CLT (Tab. 6) displayed that layup had a strong effect on parallel compressive strength while no significant influence was found for the parallel compressive modulus. Based on the results from analysis of least significant difference (summarized in Tab. 7), it could be found that thickness, the number of layers and layup orientation all had no prominent impact on the parallel compressive modulus, but they significantly affected the parallel compressive strength.

3.2 Failure Modes

3.2.1 Experimental Failure Modes

Failure modes of the four types of CLT in bending testing were shown in Fig. 3. As can be seen, for 3-layer-75, 3-layer-45 and 5-45°-layer-75 CLT, although planar shear failure occurring in the transverse layer and tensile failure occurring in the bottom layer simultaneously arose in CLT, the main failure mode for bending testing was tensile failure as shown in Figs. 3(a), 3(b) and 3(d). However, for 5-layer-75 CLT, the delamination failure of horizontal bonding surfaces emerged between the middle layer and outer layer (see Fig. 3(c)).

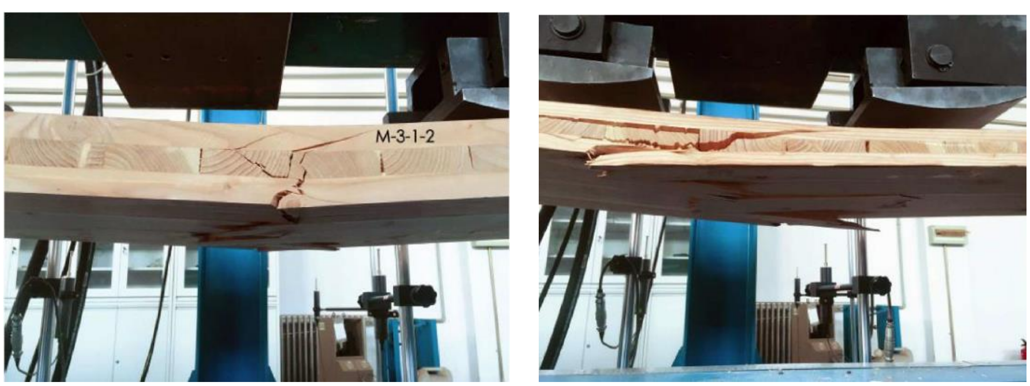

(a) (b)

(c) (d)

Figure 3: Failure modes of bending testing for: (a) 3-layer-75 CLT, (b) 3-layer-45 CLT, (c) 5-layer-75 CLT, (d) 5-45°-layer-75 CLT

Fig. 4 presented the failure modes of measured CLT for rolling shear testing. It is worthwhile to note that the main failure mode was planar shear failure.

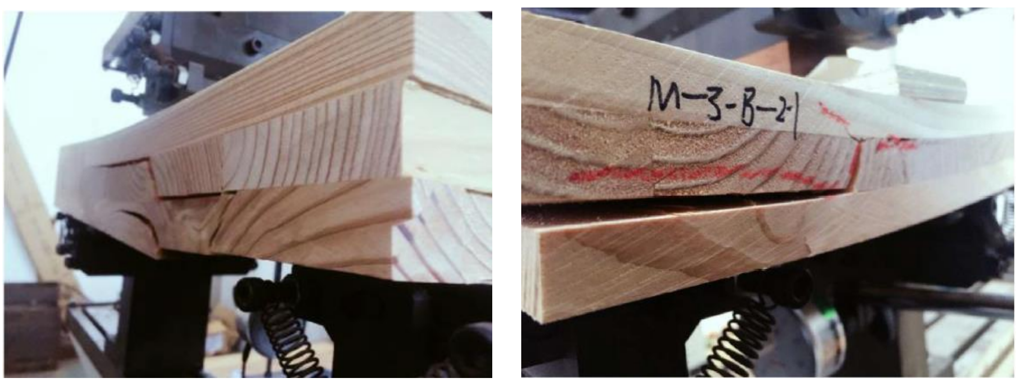

(a) (b)

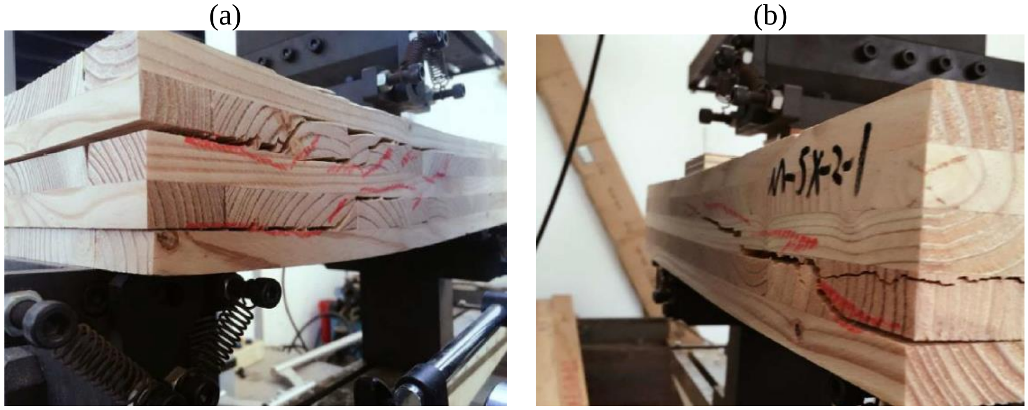

(c) (d)

Figure 4: Failure modes of rolling shear testing for: (a) 3-layer-75 CLT, (b) 3-layer-45 CLT, (c) 5-layer-75 CLT, (d) 5-45°-layer-75 CLT

Experimental failure modes of CLT for parallel compressive testing were provided in Fig. 5. As can be seen in Figs. 5(a) and 5(b), for three-layer CLT, fiber fold failure existing in the outer layer was the main failure mode. But shear failure seen in the transverse layer dominated for five-layer CLT (seen from Figs. 5(c) and 5(d)).

(a)

(b)

(c)

(d)

Figure 5: Failure modes of parallel compression testing for: (a) 3-layer-75 CLT, (b) 3-layer-45 CLT, (c) 5-layer-75 CLT, (d) 5-45°-layer-75 CLT

3.2.2 Simulated Failure Modes

Strain diagrams derived from numerical simulation of bending properties for selected CLT were illustrated in Fig. 6. It is clear that the maximum strain for bending tests was primarily from the bottom layer of CLT. Therefore, tensile failure occurring in the bottom layer should be the main failure mode for numerical simulation, which coincided with the experimental result for 3-layer-75, 3-layer-45 and 5-45°-layer-75 CLT (see Figs. 3(a), 3(b) and 3(d)). An exception was 5-layer-75 CLT, where delamination failure came out in bonding surfaces between the middle layer and outer layer and became the main failure mode. This was possibly attributed to the overestimated or undesirable bonding condition between layers of CLT. Due to the probably poor bonding condition, the adhesive force between timber layers was decreased, lower than expected strength, leading to delamination failure before the tensile failure occurred.

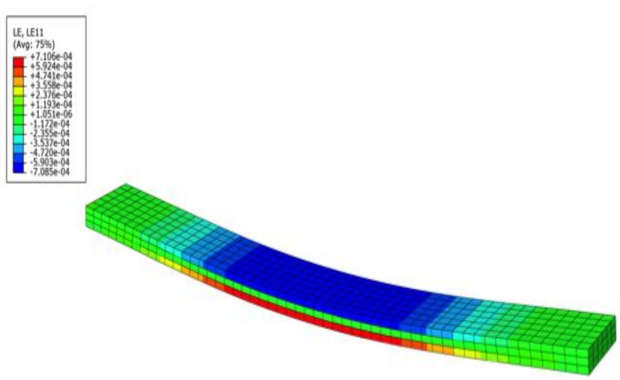

(a)

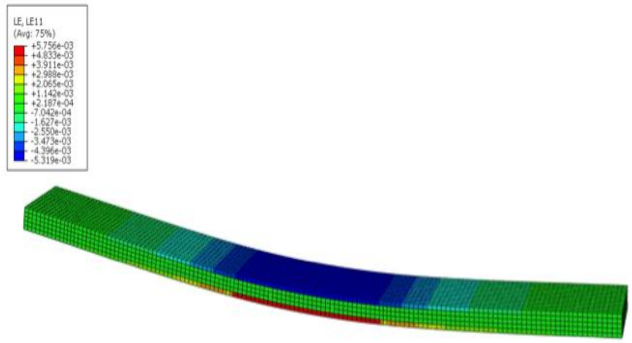

(b)

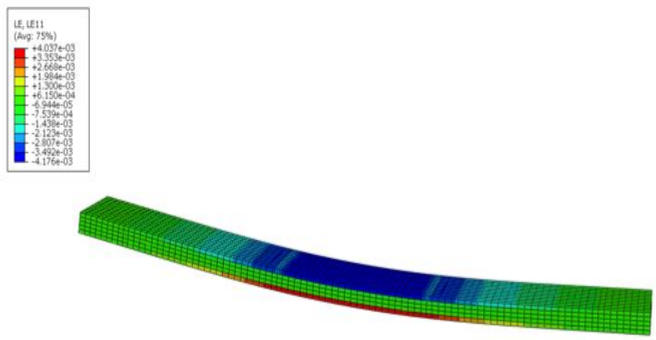

(c)

Figure 6: Strain diagram of bending properties of: (a) 3-layer-75 CLT, (b) 5-layer-75, (c) 5-45°-layer-75 CLT

Fig. 7 gave the strain diagram obtained from numerical simulation of rolling shear performance. Obviously, the maximum strain for rolling shear was concentrated in the transverse layer of three-layer or five-layer CLT, which meant that rolling shear failure happening in the transverse layer of CLT appeared to be the main failure mode for simulation. This finding was greatly in line with the experimental one (shown in Fig. 4).

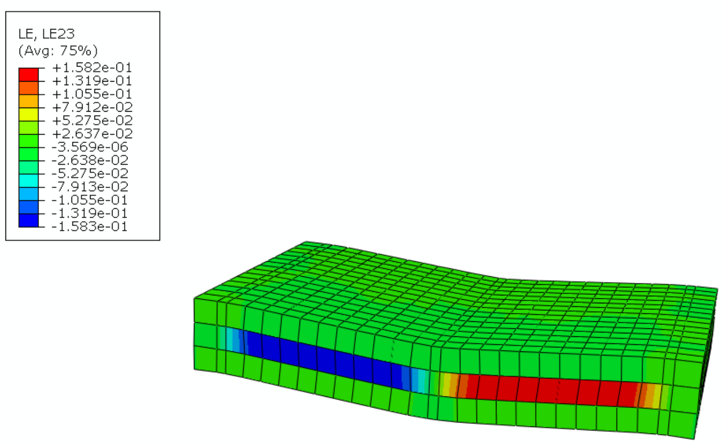

(a)

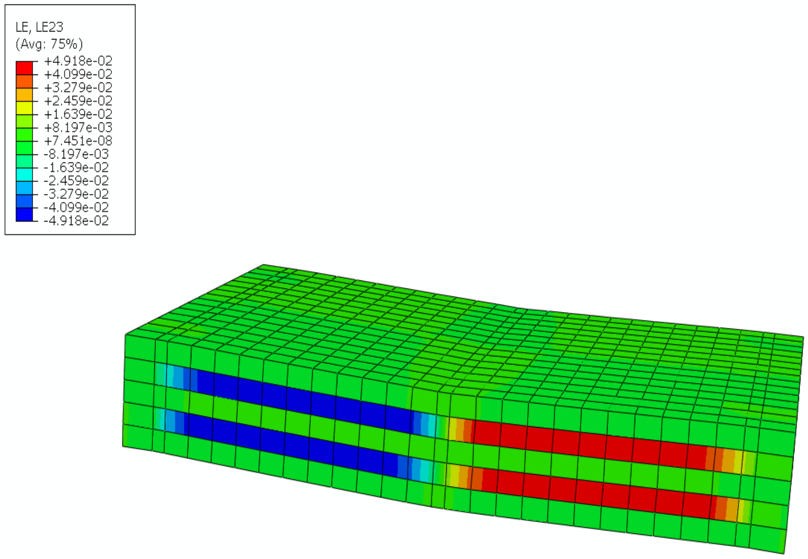

(b)

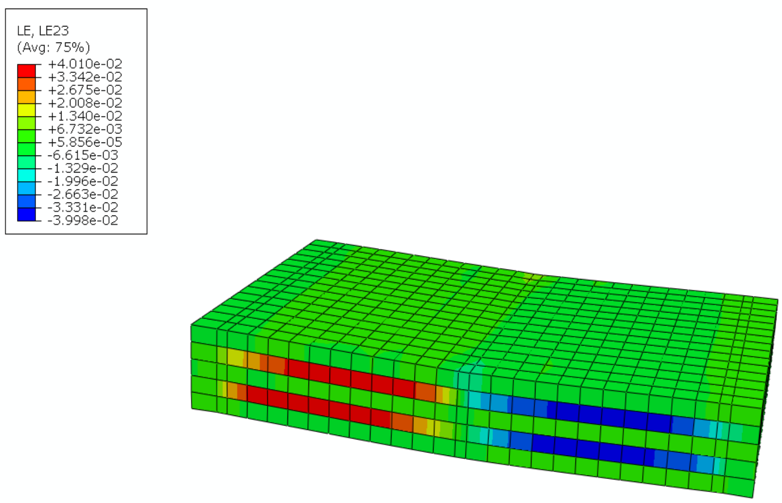

(c)

Figure 7: Strain diagram of rolling shear properties of: (a) 3-layer-75 CLT, (b) 5-layer-75, (c) 5-45°-layer-75 CLT

Similarly, the simulated maximum strain for parallel compressive came from the transverse layer of CLT, namely, rolling shear failure occurring in the transverse layer of CLT came as the main failure mode for simulation (seen in Fig. 8). This result was basically consistent with that from parallel compressive experiment for 5-layer-75 and 5-45°-layer-75 CLT. Nevertheless, it should be noted that fiber fold failure was found to be the major failure mode of parallel compressive experiment for 3-layer-75 and 3-layer-45 CLT, which was different from the results found in simulation. Further research is needed to explain the failure mode of parallel compressive test in terms of 5-layer-75 and 5-45°-layer-75 CLT.

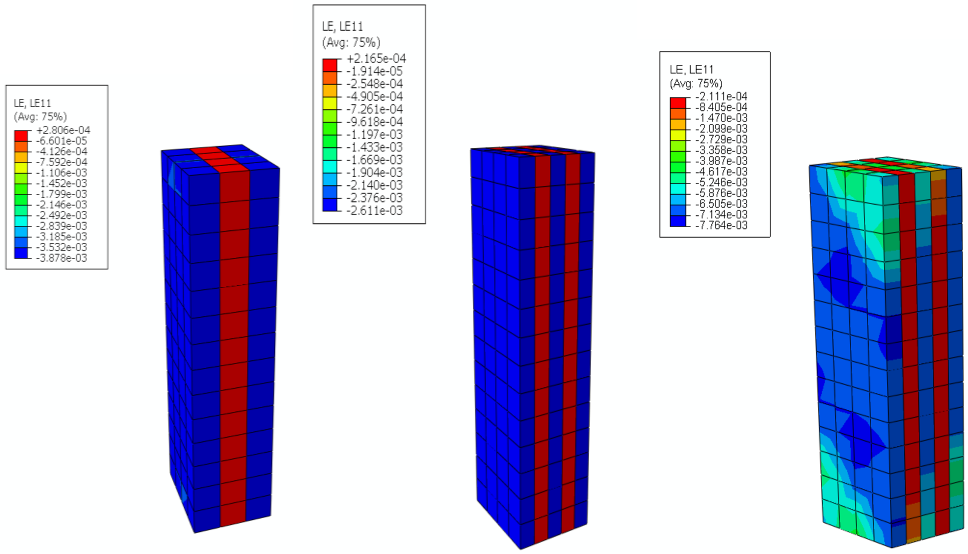

(a) (b) (c)

Figure 8: Strain diagram of parallel compression properties of: (a) 3-layer-75 CLT, (b) 5-layer-75, (c) 5-45°-layer-75 CLT

3.2.3 Prediction for Mechanical Properties of CLT

Numerical simulation results showed that the failure modes obtained by numerical simulation were basically consistent with those from experimental testing. To further verify the validity of numerical simulation, maximum failure load of CLT from the simulation was calculated and compared with that from mechanical experiment, as shown in Tab. 8. For 3-layer-75 CLT, the maximum failure load of numerical simulation for bending test was 42.10 kN and the corresponding value from lab testing was 39.33 kN, generating a 7.04% variation.

Table 8: Results of the mechanical properties for CLT based on finite element numerical simulation

CLT	Maximum failure load (kN)					
	Numerical simulation values			Tested values		
	Bending test	Rolling shear test	Compressive test	Bending test	Rolling shear test	Compressive test
3-layer-75`	42.10 (+7.04%)	82.62 (+3.96%)	255.19 (-2.54%)	39.33	79.47	261.84
5-layer-75	32.96 (-2.08%)	77.37 (+8.88%)	233.80 (+0.97%)	33.66	71.06	231.56
5-45°-layer-75	33.23 (-5.27%)	101.21 (+4.89%)	259.10 (-3.10%)	35.08	96.49	267.39

Additionally, the maximum rolling shear failure load values for simulation (82.62 kN) were 3.96% higher than those for lab tests (79.47 kN). Regarding the maximum parallel compressive failure load, 255.19 kN was found for simulation, which was just 2.54% lower than tested value, 261.84 kN. Similar results were found in both 5-layer-75 and 5-45°-layer-75 CLT. Obviously, there was a little difference between the simulated values and the measured values, because the support constraint conditions of numerical simulation were not completely the same as those of experimental tests. In general, the variation of maximum failure load obtained from simulation and lab tests for CLT was under 10% (as shown in Tab. 8). Therefore, maximum failure load values calculated from simulation were valid, and the mechanical performance of CLT could be equivalently predicted using the numerical simulation method.

3.3 Analytical Approach

Results of effective bending stiffness and effective shear stiffness calculated from Eqs. (8) and (9) for 3-layer-75, 3-layer-45 and 5-layer-75 CLT were shown in Tab. 9.

Table 9: Effective bending stiffness and effective shear stiffness of CLT with different lay-ups

CLT	Effective bending stiffness (10^9 N × mm^2/m)		Effective shear stiffness (10^6 N/m)	
	Theoretical value	Test value	Theoretical value	Test value
3-layer-75`	469.67 (+2.29%)	459.14	6.01 (-1.48%)	6.10
3-layer-45	100.44 (-1.01%)	101.45	3.80 (+5.26%)	3.61
5-layer-75	388.46 (-2.90%)	400.08	7.20 (+6.34%)	6.78

Theoretical value and test value were highly consistent for both effective bending stiffness and shear stiffness. The theoretical values of effective bending stiffness were very close to testing values for the three types of CLT. Average differences between theoretical value and test value for effective bending stiffness were +2.29%, -1.01%, and -2.90% for 3-layer-75, 3-layer-45, and 5-layer-75 CLT, respectively. For effective shear stiffness, the average variation was -1.48%, +5.26%, and +6.34%, respectively. Obviously, shear analogy method can be used to predict the mechanical properties of CLT.

4 Conclusions

The objective of this study was to evaluate the mechanical properties of CLT with different lay-ups by using fast-growing Japanese larch. The conclusions are as follows:

(1) The bending strength and modulus, rolling shear strength and modulus, and parallel compression strength and modulus of CLT all decreased with the thickness of timber. Meanwhile bending strength and modulus, and parallel compression strength and modulus increased with the number of layers. Lay-ups significantly affected on bending, rolling shear and parallel compression properties of CLT. The number of layers had a prominent impact on bending, rolling shear and parallel compression strength. Thickness and layup orientation both had a remarkable influence on rolling shear and parallel compression strength.

(2) Major failure mode for bending test was tensile failure occurring in the bottom layer of CLT. As to rolling shear testing, the main failure mode was planar shear failure. Fiber fold failure was the main failure mode for parallel compression testing. Failure modes obtained from numerical simulation were basically in line with those from experimental test.

(3) There was strong alignment between theoretical value and test value for effective bending stiffness and shear stiffness. The shear analogy method can be used to predict the mechanical properties of CLT effectively.

Acknowledgement: This research was funded by basic operating budget of scientific research institutes for public welfare at the central level (CAFBB2018SY032) and China Postdoctoral Science Foundation (No. 2018M641225).

References

1. Stürzenbecher, R., Hofstetter, K., Eberhardsteiner, J. (2010). Structural design of cross laminated timber (CLT) by advanced plate theories. *Composites Science and Technology, 70(9),* 1368-1379.
2. Laguarda, F., Espinoza, O. (2015). Awareness perceptions and willingness to adopt cross-laminated timber by the architecture community in the United States. *Journal of Cleaner Production, 94,* 198-210.
3. Davids, W. G., Willey, N., Lopez-Anido, R., Shaler, S., Gardner, D. et al. (2017). Structural performance of hybrid SPFs-LSL cross-laminated timber panels. *Construction and Building Materials, 149,* 156-163.
4. Wang, Z. Q., Luo, D., Zheng, W., Yao, Y., Lu, X. N. (2017). Effect of hybrid structure on lateral load resistance of cross-laminated timber shear wall. *Journal of Structural Engineering, 2(2),* 145-151.

5. Gsell, D, Feltrin, G, Schubert, S. (2007). Cross-laminated timber plates: evaluation and verification of homogenized elastic properties. *Journal of Structural Engineering, 133(1),* 132-138.
6. Park, H. M., Fushitani, M., Sato, K. (2003). Static bending strength performances of cross-laminated woods made with five species. *Journal of Wood Science, 49(5),* 411-417.
7. Wang, Z. Q., Zhou, J. H., Dong, W. Q., Yao, Y., Gong, M. (2018). Influence of technical characteristics on the rolling shear properties of cross laminated timber by modified planar shear tests. *Maderas Cienciay Tecnología, 20,* 469.
8. Karacabey, E., Douglas, B. (2013). *Cross-laminated timber handbook*. FPInnovations, Quebec, Canada.
9. Li, H. T., Qiu, Z. Y., Wu, G., Wei, D. D., Lorenzo, R. et al. (2019). Compression behaviors of parallel bamboo strand lumber under static loading. *Journal of Renewable Materials, 7(7),* 583-600.
10. Li, H. T., Qiu, Z. Y., Wu, G., Corbi, O., Wei, D. D. et al. (2019). Slenderness ratio effect on eccentric compression performance of parallel strand bamboo lumber columns. *Journal of Structural Engineering ASCE, 145(8),* 04019077.
11. Zhou, Q., Gong, M., Ying, H. C., Mohammad, M. (2014). Measurement of rolling shear modulus and strength of cross laminated timber fabricated with black spruce. *Construction and Building Materials, 64,* 379-386.
12. Gong, Y. C., Wu, G. F., Ren, H. Q. (2016). Block shear strength and delamination of Cross-Laminated Timber fabricated with Japanese larch. *BioResources, 11(4),* 10240-10250.
13. Fu, H. M., Wang, Z. Q. (2014). Application and development prospect of Cross-laminated Timber. *Forestry Machinery & Woodworking Equipment, 50(1),* 68-81.
14. Shen, Y. L., Schneider, J., Tesfamariam, S., Stiemer, S. F., Mu, Z. G. (2013). Hysteresis behavior of bracket connection in cross-laminated-timber shear walls. *Construction and Building Materials, 48,* 980-991.
15. Schneider, J., Shen, Y., Stiemer, S. F., Tesfamariam, S. (2015). Assessment and comparison of experimental and numerical model studies of cross-laminated timber mechanical connections under cyclic loading. *Construction and Building Materials, 77,* 197-212.
16. Saaveda, E. I., Saavedra, K., Hinojosa, J., Chandra, Y., Das, R. (2015). Multi-scale modelling of rolling shear failure in cross-laminated timber structures by homogenization and cohesive zone models. *International Journal of Solids & Structures, 81,* 219-232.
17. Li, Y., Lam, F. (2015). Reliability analysis and duration-of-load strength adjustment factor of the rolling shear strength of cross laminated timber. *Journal of Wood Science, 62(6),* 1-11.
18. Zhou, Q. Y., Gong, M., Chui, Y. H., Mohammad, M. (2014). Measurement of rolling shear modulus and strength of cross-laminated timber using bending and two-plate shear tests. *Wood & Fiber Science Journal of the Society of Wood Science & Technology, 46,* 259-269.
19. Standard for performance-rated cross-laminated Timber, ANSI/APA PGR320-2017 (2017).
20. Standard test methods of static tests of lumber in structural sizes, ASTM D198-02 (2002).
21. Standard test methods for mechanical properties of lumber and wood base structural material, ASTM D4761-13 (2013).
22. Etienne, A., Pascal, L., Luigi, M. (2011). The modal stability procedure for dynamic and linear finite element analysis with variability. *Finite Elements in Analysis and Design, 47(1),* 30-45.
23. Joel, M., Lei, X. (2011). Simplified nonlinear finite element analysis of buildings with CFS shear wall panels. *Journal of Constructional Steel Research, 67(4),* 565-575.
24. Li, W. J. (1983). Elasticity and drying stresses of wood. *Journal of Nanjing Technological College of Forest Products, 6,* 115-122.
25. Sliker, A. (1985). Orthotropic strains in compression parallel to grain tests. *Forest Products Journal, 35(11),* 19-26.
26. Sliker, A. (1989). Measurement of the smaller Poisson ratios and related compliances for wood. *Wood & Fiber Science Journal of the Society of Wood Science & Technology, 21,* 252-262.
27. Gong, M. (1995). A study of wood elastic parameters parallel to grain in compression test by using resistance strain gauges. *Scientia Silvae Sinicae, 31(2),* 190-191.
28. Wang, Z., Gong, M., Chui, Y. H. (2015). Mechanical properties of laminated strand lumber and hybrid cross-laminated timber. *Construction and Building Materials, 101,* 622-627.

29. Daniel, P. H., John, C. B. (2014). Mechanical properties of southern pine Cross-Laminated Timber. *Journal of Materials in Civil Engineering, 27(9),* 401-425.
30. Simon, A., Zachary, C., Maren, H. (2016). Rolling shear modulus and strength of beech wood lamination. *Holzforschung, 70,* 773-781.
31. Gong, M., Tu, D. Y., Li, L., Chui, Y. H. (2015). Interlaminar shear properties of hardwood cross layer in hybrid cross laminated timber. *Proceedings of the 5th International Scientific Conference on Hardwood Processing*.
32. Wang, Z. Q., Fu, H. M., Gong, M. (2017). Planar shear and bending properties of hybrid CLT fabricated with lumber and LVL. *Construction & Building Materials, 151,* 172.
33. Gu, M. Z., Pang, W. C. (2016). Rolling shear strengths of Southern Pine cross laminated timber, wood design focus. *Wood Design Focus-Forest Products Society, 26,* 25-33.
34. Wang, Z. Q., Dong, W. Q., Wang, Z. Z., Zhou, J. H., Gong, M. (2018). Effect of macro characteristic on rolling shear properties of fast-growing poplar wood laminations. *Wood Research, 63(2*), 227-238.